Validation of a New Analytical Formula to Predict the Steel Temperature of Heavily Insulated Cross-Sections

Luca Possidente, Department of Civil, Environmental & Geomatic Engineering, University College London, London, UK

Nicola Tondini ⓘ **, Department of Civil, Environmental and Mechanical Engineering, University of Trento, Via Mesiano 77, 38123 Trento, Italy*

Abstract. Fire protection is a popular solution to slow down the temperature increase in steel elements subjected to fire, and simple equations, such as the mass lumped formula proposed in EN1993-1-2, may be employed to estimate the steel temperature in the cross-section. The EN1993-1-2 formula assumes that the temperature of the exposed insulation surface and the surrounding gas are equal. This simplification may provide inaccurate results for heavily insulated steel sections. Therefore, a new mass lumped formula was derived, accounting for more accurate boundary conditions considering the heat flux impinging the insulation. On these premises, this work evaluates how the new simple formula fares with respect to the EN1993-1-2 formula. In this respect, a comprehensive comparison with the results of 1-D and 2-D analyses considering several insulation materials and thicknesses of insulation and steel is thoroughly presented. The proposal results in being always safe and better estimates steel temperatures relevant in the structural fire engineering context. Its use is particularly recommended for heavily insulated sections, where the ratio between the insulation and the steel heat capacities is higher than 14, and the EN1993-1-2 formula gives unsafe predictions.

List of Symbols

A	Exposed area (m²)
A_{st}	Exposed steel area (m²)
c	Specific heat capacity (J/kgK)
c_{in}	Specific heat capacity of insulation (J/kgK)
c_{st}	Specific heat capacity of steel (J/kgK)
C	Heat capacity (J/m²K)
C_{st}	Heat capacity of steel (J/m²K)
C_{st+in}	Heat capacity of the insulation-steel system (J/m²K)
d_{in}	Insulation thickness (m)
d_{st}	Steel thickness (m)

---
* Correspondence should be addressed to: ; Nicola Tondini, E-mail: nicola.tondini@unitn.it

h_c	Convection heat transfer coefficient (W/m²K)
h_r	Radiation heat transfer coefficient (W/m²K)
h_{tot}	Total heat transfer coefficient (W/m²K)
k_{in}	Thermal conductivity of insulation (W/mK)
k_{st}	Themial conductivity of steel (W/mK)
$\dot{q}''_{tot}$	Total heat flux (W/m²)
$\dot{q}''_{inc}$	Incident radiation (W/m²)
R_{in}	Heat transfer resistance of insulation (K m²/W)
R_h	Total heat transfer resistance (K m²/W)
R_{h+in}	Total heat transfer resistance considering insulation (Km²/W)
R_r	Radiative lie at transfer resistance (K m²/W)
t	Tune (s)
T	Temperature (C) or (K)
T_f	Fire temperature (C) or (K)
T_g	Gas temperature (C) 0r (K)
T_s	Exposed surface temperature (C) or (K)
T_{st}	Steel temperature (C) or (K)
$T_{st,FEM}$	Numerical steel temperature (C) or (K)
T_r	Radiative temperature (C) or (K)
V	Volume of the solid (m³)
V_{st}	Volume of the steel (m³)
ε_{in}	Emissivity of insulation (-)
ε_s	Surface emissivity (-)
μ	Ratio between insulation and steel capacities (−)
ρ	Specific heat density (kg/m³)
ρ_{in}	Specific heat density of insulation (kg/m³)
ρ_{st}	Specific heat density of steel (kg/m³)
σ	Stefan-Boltzmann coefficient (W/m²K⁴)

1. Introduction

Passive fire protection is still the most widespread solution to comply with the fire safety requirements of a steel structure. Indeed, since steel members are vulnerable to thermal attack owing to high thermal conductivity and the small thickness of the cross sections, fire verification may be particularly demanding, and insulation is a viable option to slow down the temperature increase in the elements without modifying the original structural design. In fact, the fire design of unprotected steel members may govern the dimensions of the cross sections. There may be exceptions; for instance, structures that are designed to withstand significant accidental actions, such as buildings located in regions with high seismicity [1, 2]. Consequently, thermal insulation of steel structures has attracted the interest of many researchers [3–10]. In greater detail, a review of existing fire protections with their advantages and disadvantages was published by The National Institute of Standards and Technology (NIST) [3], while Leborgne and Thomas [4] focused on the presentation of three typical fire protection systems: intumescent paints, sprayed-based protections and board systems. A literature review and an experimental campaign on intumescent coatings were presented in [5] and [6], while a numerical-based investigations for gypsum plasterboard panels was described in [7]. Moreover, new applications or patented solutions were developed in the last decades [8–10]. Concrete encasements and brick walls may also be employed as

protective solutions because they are characterised by high insulation capacity. In this respect, several experimental studies were carried out on encased steel sections, in which concrete also provides fire protection to the inner steel core [11–14].

In this context, despite the continuous improvement of computer capabilities and the development of advanced numerical tools such as finite element modelling [15, 16], easy-to-use hand calculations or spreadsheets are still valuable due to the flexibility required in the design process and for a quick assessment of the suitable fire protection to comply with the fire resistance requirements. Moreover, numerical simulations entail the knowledge and the selection of several parameters that are not straightforward for non-expert users, such as the mesh and time step size and coefficients for the numerical solver. Predictive analytical formulas belong to these simple methods that are beneficial because engineers and researchers are able to rapidly estimate the temperature of insulated steelwork without performing in-depth numerical thermal analyses. As a result, a predictive formula was developed [17] and included in the Eurocodes for the fire design of steel (EN1993-1-2 [18]) and steel–concrete composite structures (EN1994-1-2 [19]). For simplicity, this formula is hereafter referred to as the EN1993-1-2 formula. Referring to the formulation proposed in [17] and to the ECCS recommendations [20], Melinek and Tomas [21] used the Laplace transform to define an effective time delay term t_d for the EN1993-1-2 formula. This time delay term accounts for the retardant effect of insulation, which delays the steel temperature increase. The same time delay t_d identified in [21] was also suggested in [22] for insulation materials with high heat capacity C, which typically consist of materials with high density, such as bricks or concrete. In addition, Wong and Ghojel [23] highlighted that for insulation materials with relatively high density and high conductivity, the total heat transfer coefficient h_{tot}, that accounts for convection and radiation, should be accurately considered, because the EN1993-1-2 formula does not provide accurate predictions. Indeed, a Dirichlet boundary condition is typically assumed by assigning to the exposed surface the temperature of adjacent gas $T_s(t, x = x_0) = T_g(t)$, albeit a more realistic condition on the total heat flux received by the surface $-k \cdot \frac{\partial T_s}{\partial x}\big|_{x=x_0} = \dot{q}''_{tot}$ should be preferred.

This paper thoroughly validates a new simple analytical formula based on the mass lumped approach to estimate insulated steel element temperature. The formula is derived from a heat flux boundary condition on the exposed insulation surface that considers radiative and convective components. Therefore, the explicit evaluation of the total heat transfer coefficient h_{tot} is required at each time step of the calculation. To keep the proposed new formula simple, the terms that account for the time delay are neglected. Numerical results of a parametric study based on 1-D heat transfer finite element analyses were employed to investigate the accuracy of the formula predictions. Moreover, a comparison with the formula currently prescribed in EN1993-1-2 was also performed. Finally, predictions of the new proposal and EN1993-1-2 formulas were also compared with results of 2-D heat transfer finite element analyses of relevant applications and experimental data.

2. Analytical Formulas to Evaluate the Temperature of Insulated Steelwork

This section presents the new formula and briefly recalls the recursive equation prescribed in the current EN1993-1-2 and EN1994-1-2.

2.1. New Formula

Here a brief recall of the derivation of the new formula is provided. At the same time, interested readers can find the complete derivation in a dedicated paper [24] and additional details on the basics of heat transfer in several textbooks [25–27]. Since steel has a very high thermal diffusivity, it can be assumed that the temperature is uniform in sufficiently thin sections, and all the section heat can be lumped into a zero-dimension point. Thus, the temperature becomes only time-dependent. Considering the contributions by radiation and convection separately, the total received heat flux $\dot{q}''_{tot}$ by the steel surface can be written as

$$\dot{q}''_{tot} = \varepsilon_s \dot{q}''_{inc} - \varepsilon_s \sigma T_{st}^4 + h_c(T_g - T_{st}) = \varepsilon_s \sigma(T_r^4 - T_{st}^4) + h_c(T_g - T_{st}) \tag{1}$$

with ε_s the target surface emissivity, $\dot{q}''_{inc}$ the incident radiation, $\sigma = 5.67 \cdot 10^{-8}$ W/(m^{2}K^4) the Stefan-Boltzmann constant, h_c the convection heat transfer coefficient and $T_r \equiv \sqrt[4]{\dot{q}''_{inc}/\sigma}$ the effective radiation temperature. Assuming $T_r = T_g = T_f$, which is a typical simplification for fully-developed fires, the rate of steel temperature increase, considering the equilibrium between the total received heat flux $\dot{q}''_{tot}$ by the exposed area A in a time dt and the heat stored in the volume V, can be expressed as follows

$$\frac{dT_{st}}{dt} = \frac{A}{V \cdot \rho \cdot c} \dot{q}''_{tot} = \frac{\dot{q}''_{tot}}{C} = \frac{(T_f - T_{st}) \cdot (h_r + h_c)}{C} = \frac{(T_f - T_{st}) \cdot 1/R_h}{C} \tag{2}$$

where ρ is the density, c is the specific heat capacity and $C = (V/A) \cdot \rho \cdot c$ is the heat capacity of the heated solid, while $h_r = \varepsilon_s \sigma(T_f^2 + T_{st}^2)(T_f + T_{st})$ is the radiation heat transfer coefficient and R_h the total heat transfer resistance.

For insulated steel sections the contribution of the insulation material should be computed and R_h in Equation (2) should be substituted with R_{h+in}

$$R_{h+in} = R_h + R_{in} = \frac{1}{h_r + h_c} + \frac{d_{in}}{\lambda_{in}} \tag{3}$$

A contribution of the insulation material to the total heat capacity, particularly relevant for heavily insulated steel sections, should also be accounted

$$C = C_{st} + \chi C_{in} \tag{4}$$

Although the contribution of the insulation capacity may vary depending on parameters, such as the temperature T and the material properties, for simplicity, a constant χ value is assumed. Numerical analyses, later discussed in Sect. 3, showed that adding half of the heat capacity of the insulation to the total heat capacity ($\chi = 0.5$) provides good and conservative predictions. It should be observed that for 1-D applications, the section factor V_{st}/A_{st} of the steel cross section is equivalent to the steel thickness d_{st} and therefore $C_{st} = (V_{st}/A_{st}) \cdot \rho \cdot c = d_{st} \cdot \rho \cdot c$. Finally, the proposed formula is obtained by substituting Equations (3) and (4) in (2), where the time derivative of temperature is approximated as $\frac{dT}{dt} \approx \frac{\Delta T}{\Delta t}$. Then, by assuming constant the time increment $\Delta t = t_{i+1} - t_i$ between two consecutive steps i and $i+1$, it reads

$$T_{st}^{i+1} = T_{st}^i + \frac{1}{\left(C_{st} + \frac{d_{in}\rho_{in}c_{in}}{2}\right)} \frac{1}{\left(\frac{1}{h_{tot}^i} + \frac{d_{in}}{\lambda_{in}}\right)} \left(T_f^i - T_{st}^i\right)\Delta t$$

$$\text{with } h_{tot}^i = h_r^i + h_c = 4\varepsilon_{in}\sigma\left(T_f^i\right)^3 + h_c \tag{5}$$

in which, differently from EN 1993-1-2, the simplification $T_{st} = T_f$ was accepted only for the h_r^i term in Equation (5) since, as confirmed by numerical analyses, no significant variation in the T_{st} predictions is introduced. Note that if temperature-dependent material properties are assumed, they should be updated at each step, as for $c_{st}^i = c_{st}(T_{st}^i)$.

2.2. The EN1993-1-2 Formula

According to EN1993-1-2 [18], for a uniform temperature distribution in the cross-section, the temperature T_{st}^{i+1} of an insulated steel member induced by a temperature increase ΔT_{st}^{i+1} during the time interval $\Delta t = t_{i+1} - t_i$ should be obtained as follows

$$T_{st}^{i+1} = T_{st}^i + \Delta T_{st}^{i+1} = T_{st}^i + \frac{\lambda_{in}A_{st}/V_{st}}{d_{in}c_{st}\rho_{st}} \frac{\left(T_f^i - T_{st}^i\right)}{\left(1 + \frac{\mu}{3}\right)}\Delta t - \left(e^{\frac{\mu}{10}} - 1\right)\Delta T_f^{i+1}$$

$$\text{with } \Delta T_{st}^{i+1} \geq 0 \ \text{if } \Delta T_f^{i+1} = T_f^{i+1} - T_f^i > 0 \tag{6}$$

where the parameter μ is calculated as

$$\mu = \frac{c_{in}\rho_{in}}{c_{st}\rho_{st}}d_{in}\frac{A_{st}}{V_{st}} \tag{7}$$

As aforementioned, this formula was derived by assuming a Dirichlet boundary condition in the heat transfer equations, assigning to the exposed surface the fire

temperature $T_f(t)$. The time delay t_d is accounted in the exponential term of Equation (6) and, as prescribed in EN1993-1-2, the value of Δt should not be greater than 30 s.

3. Validation of the New Formula

In this section, the new and the EN1993-1-2 formulas are compared against the numerical results of a parametric study, consisting of 1-D thermal analyses of insulated steel sections. First, the parametric study and the numerical model implemented in SAFIR [28] are presented. Then, numerical outcomes and predictions from the two formulas are compared. Finally, the range of applicability and a possible improvement of the proposed new formula are described.

3.1. Parametric 1-D Heat Transfer Analysis

In order to investigate the accuracy and the applicability range of the new proposed and the EN1993-1-2 formula, a parametric study consisting of 1-D thermal analyses was carried out. Indeed, both the heat flux applied to the boundary conditions and the model representing the insulation and the steel material are such that the problem is one-dimensional. 10 insulation materials with different properties were investigated, as reported in Table 1. The insulation thickness was varied in a range relevant to each insulation material. In greater detail, nine d_{in} values were investigated. In this respect, for all the materials except for the bricks, a minimum thickness value of 10 mm and a maximum thickness value of 50 mm at 5 mm increments were selected, whereas for the bricks a minimum thickness value of 100 mm and a maximum thickness value of 300 mm at 25 mm increments were chosen. Given the distribution of the thickness of plates composing H and I steel sections, fifteen values of steel thickness d_{st} were selected, as reported in Fig. 1 and in Table 1.

The numerical simulations were performed through the finite element software SAFIR [28]. Quadrangular finite elements with linear shape functions were employed. The 1-D model consisted of an insulation layer exposed on the upper surface, and a steel layer with an adiabatic condition at the bottom surface. Adiabatic conditions, imposed on the lateral surfaces, allowed for the development of a 1-D heat flux through the thickness and the width of the insulated steel element did not influence the thermal distribution. However, to ensure similar discretisation and numerical convergence in all the analyses, the width was conventionally set equal to 1.25 times the total thickness of the element $d_{in} + d_{st}$ in all the investigated configurations. The total heat flux $\dot{q}''_{tot}$ associated with the ISO834 heating curve was applied as a boundary condition on the exposed surface

$$\dot{q}''_{tot} = \varepsilon_s \cdot \sigma \cdot (T_f^4 - T_s^4) + h_c \cdot (T_f - T_s) \tag{8}$$

Table 1
Investigated Insulation Materials [29] and Steel Thicknesses

|	ρ_{in}(kg/m^3)	λ_{in}(W/mK)	c_{in}(J/kgK)	d_{in}(mm) range
Calcareous concrete	2200	1.30	1200	10–50
Concrete with voids	600	0.30	1200	10–50
Lightweight concrete	1600	0.80	1200	10–50
Siliceous concrete	2400	1.70	1200	10–50
Mineral fibres	250	0.10	1100	10–50
Gypsum boards	800	0.20	1700	10–50
Rockwool	120	0.25	1100	10–50
Silicate boards	450	0.15	1100	10–50
Bricks	2000	1.00	1200	100–300
Vermiculite	300	0.15	1100	10–50
Steel thickness d_{st} (mm)	3, 5, 8, 10, 13, 16, 18, 21, 24, 26, 29, 32, 34, 37, 40			
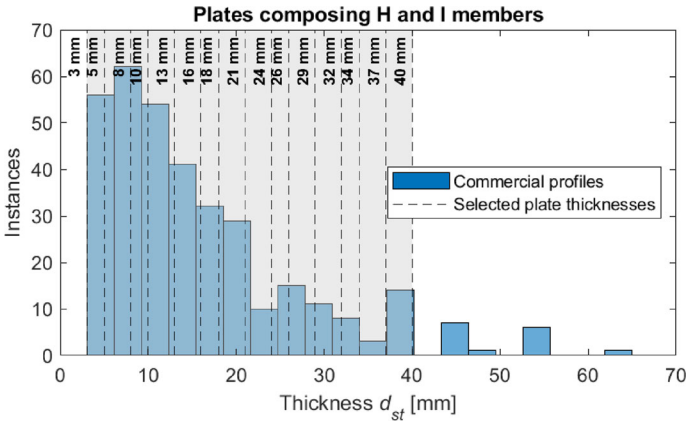
Figure 1. Thickness of plates composing commercial H and I steel profiles.

where T_s and $\varepsilon_s = \varepsilon_{in}$ are the temperature and the emissivity of the exposed insulation surface and the fire temperature T_f is the temperature prescribed by the ISO834 heating curve

$$T_f = 20 + 345 \; \log_{10}(8t + 1) \qquad (9)$$

with T_f and t expressed in °C and minutes, respectively. Note that hereafter super- or subscripts referring to the i-th step of analysis are omitted for simplicity. A fire exposure of 360 min was applied because it represents the highest fire resistance requirement for current standards, such as the Italian Fire Prevention Code [30]. A time step Δt equal to 10 s was used in the analyses. To have finite elements with comparable dimensions, the material with the smallest thickness was discre-

tised with 4 finite elements in each analysis. In contrast, the other material was modelled with a variable number of finite elements, as shown in Fig. 2a. Based on a mesh sensitivity analysis, the selected discretisation was a good compromise between the accuracy of the steel temperature predictions and the computational time. For instance, preliminary analyses showed that by employing twice the number of elements, the maximum steel temperature differed by less than 2.5°C. The boundary conditions and the discretisation of the numerical model for a case in which $d_{in} < d_{st}$ are shown in Fig. 2a.

The insulation material properties are reported in Table 1, whereas the additional relevant model properties are summarised in Table 2. The specific heat c_{st} and the thermal conductivity λ_{st} of steel varied with the steel temperature T_{st}, according to EN1993-1-2 [18].

As depicted in Fig. 2b, temperature gradients mainly establish in the insulation, and the steel temperature distribution is essentially uniform, confirming that a single temperature in the cross-section is a good approximation. Nevertheless, since the steel temperature is not perfectly uniform through the thickness, the temperature $T_{st,FEM}$ later compared with the predictions from the two investigated formulas, was determined as the maximum steel temperature, located at the steel-insulation interface.

3.2. *Numerical Results*

The results of the parametric analyses were collected in terms of the maximum steel temperature $T_{st,FEM}$ at each time of analysis t and were compared with the predictions of the steel temperature T_{st} obtained with the EN1993-1-2 and the new simple formula at the same analysis step. A time increment of $\Delta t = 10$ s was used both in the numerical analyses and the two simple formulas. Considering that the bisector line identifies the perfect match between predictions and FE results, Fig. 3a shows that the EN1993-1-2 provisions may be both safe (data above the bisector line) and unsafe (data below the bisector line), with the predicted steel temperature that can be significantly higher than the + 10%, or lower than the -10% of the corresponding FE temperature. The new simple analytical formula provides better predictions, that are much well distributed in the ± 10% range, particularly for steel temperatures higher than 600°C, as depicted in Fig. 3b. Predictions are unsafe for more than 10% of $T_{st,FEM}$ only for very low temperatures and never for a difference higher than 20°C and thus, are not particularly relevant for structural fire engineering applications. In fact, an initial overestimation is found at low temperatures, but predictions gradually improve when the steel temperature increases.

A reference critical temperature T_{crit} was then selected within the 400°C≤T_{st}≤800°C range, which is representative of the failure of steel elements in fire [31–33]. In this work, T_{crit} was conventionally assumed equal to 550°C, which entails a reduction of the yield strength at elevated temperature of 62.5% [18]. When T_{crit} is reached in the numerical models, the new proposal (Fig. 3b) provides conservative predictions between 549°C and 626°C (0% to + 14% of T_{crit}). Conversely, the
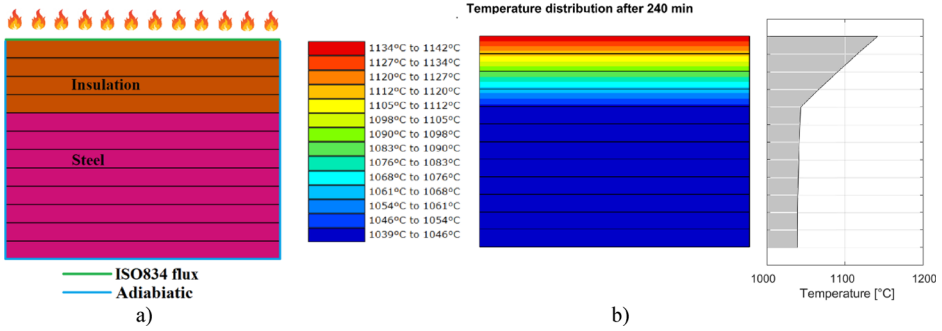
Figure 2. SAFIR analyses: (a) numerical model; (b) temperature distribution after a 240 min of fire exposure.

Table 2
Main Model Properties

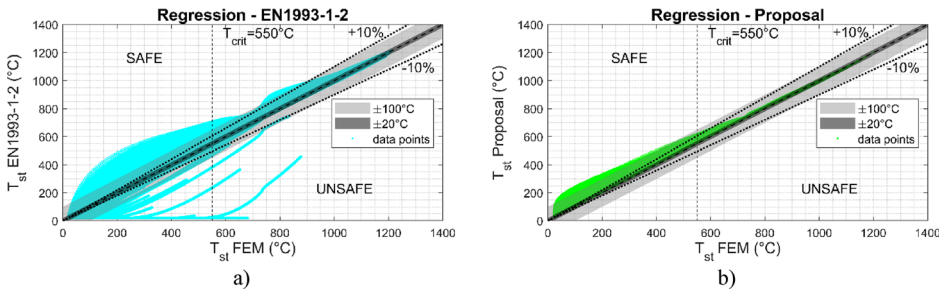| Additional properties			
Heat transfer coefficient h_c (W/m^{2}K)	25	Specific heat of steel c_{st} (J/kgK)	$c_{st} = c_{st}(T_{st})$[18]
Emissivity of steel ε_{st}	0.7	Thermal conductivity of steel λ_{st} (W/mK)	$\lambda_{st} = \lambda_{st}(T_{st})$[18]
Emissivity of insulation ε_{in}	0.9	Unit mass of steel (kg/m^3)	7850

Figure 3. Predicted steel temperatures vs numerical results: (a) EN1993-1-2 ((b)) new simple formula.

EN1993-1-2 formula (Fig. 3a) predicts steel temperatures between 20°C and 706°C, that entail larger errors (-96% to + 28% of T_{crit}).

The absolute error, evaluated as the difference between the numerical and the predicted steel temperatures, is depicted in Fig. 4. Considering all the predictions, the proposed new formula ensures, compared with the EN1993-1-2, higher frequencies of occurrence in the ranges −10°C to 0°C and the 0°C to + 10°C, and as already mentioned, never gives unsafe predictions for more than 20°C (Fig. 4b).
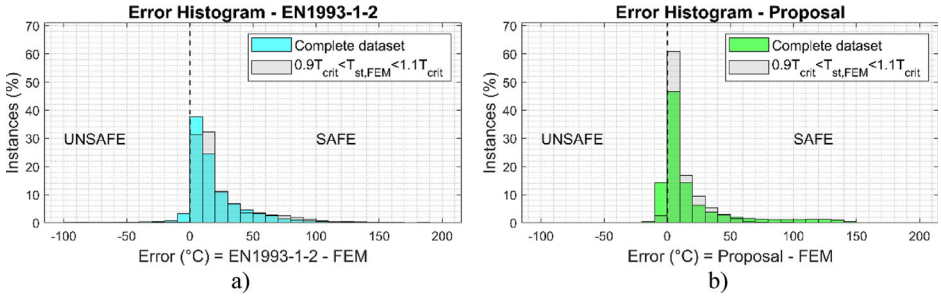
Figure 4. Prediction error distribution: (a) EN1993-1-2; ((b)) proposed new formula.

Since this formula provides very conservative values for low steel temperatures, frequencies of occurrence higher than 1% are found until an error of $+150°C$ is reached. However, limiting the analysis to the data within the relevant range $0.9T_{crit} < T_{st} < 1.1T_{crit}$, the frequencies of occurrence related to an error larger than $+70°C$ are negligible. For the EN1993-1–2 formula (Fig. 4a), more unsafe predictions are found for an error $< -10°C$. Furthermore, higher frequencies of occurrence are observed for safe predictions in the $10°C$ to $80°C$ range. The error distribution in the $0.9T_{crit} < T_{st} < 1.1T_{crit}$ range does not significantly differ from the one of the full dataset. It is worth mentioning that the error distribution of the proposed new formula has a larger tail and appears to be skewed right. This is mainly caused by overconservative predictions in the $20°C–100°C$ range, which is nevertheless not relevant in the context of structural fire engineering.

As a final observation, Fig. 5 shows the values of the root mean square error (RMSE) as a synthetic indicator of the reliability of the different formulas that reads

$$\text{RMSE} = \sqrt{\frac{\sum_{j=1}^{N}\left(T_{st,j} - T_{st,FEM,j}\right)^2}{N}} \tag{10}$$

With N the total number of predictions ($N = 10·9·15·360·60/10 = 2.916·10^6$ for the complete dataset) and j the subscript indicating the *j-th* predicted or numerical temperature. To represent the RMSE error, three relevant thresholds ($100°C$, $400°C$ and $T_{crit} = 550°C$) were identified. The first two represent the temperatures for which the Young's modulus E and the yield strength f_y of steel start degrading [18]. Indeed, while failure is unlikely for temperatures lower than $100°C$, loss of load-bearing capacity is typically observed above $400°C$ owing to the steel mechanical property degradation. In Fig. 5, the RMSE error of the new formula significantly drops for steel temperatures above the three thresholds. This confirms that inaccurate estimates are mainly obtained at low temperatures. The EN1993-1-2 formula always shows higher RMSE values, which are larger than $30°C$ for all the considered thresholds.
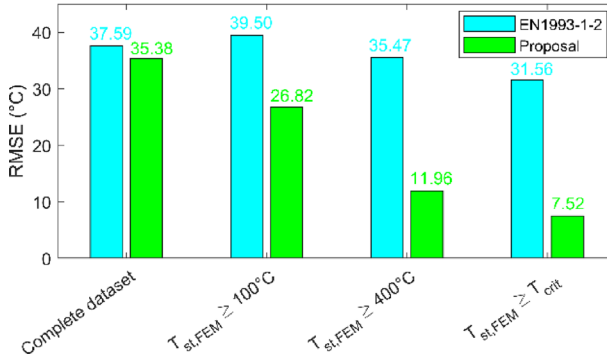
Figure 5.   RMSE comparison.

3.3. Range of applicability

In this section, the range in which the use of the proposed new formula is particularly suitable to predict the steel temperature of insulated cross sections, is identified. On these premises, Fig. 6 illustrates the ratio between predictions and numerical results as a function of μ, that represents the ratio between the heat capacities of the insulation and the steel (see Equation (7)). High μ values correspond to heavily-insulated steel sections. Predictions associated with numerical steel temperatures above the aforementioned three temperature thresholds are highlighted in Fig. 6 with different colour shades. Each point in Fig. 6 represents the temperature for a single steel-insulation configuration at a given time step. Since in the FE simulation the variation of the specific heat c_{st} with the steel temperature was considered, the value of μ varies at each time step. However, for graphical clarity the constant value, $c_{st} = 460$ J/kgK was considered to represent the data in Fig. 6. Hence, for each analysis a unique μ value is derived according to Equation (7) and results are disposed in vertical lines. In addition, a constant value of μ is easier to determine in hand-calculations, allowing for more straightforward indications about the application range of the formula.

In Fig. 6a, it is possible to observe that the EN1993-1-2 formula is particularly sensitive to μ, which denotes a marked change in the ability to provide safe predictions. Indeed, the EN1993-1-2 formula moves from being safe to unsafe in the $3 < \mu < 14$ range. On the contrary, Fig. 6b shows that the new simple formula always provides safe or slightly unsafe predictions. This formula is, in general, less precise as the variability in the prediction ratio, defined as the difference between the maximum and the minimum $T_{st}/T_{st,FEM}$ value for a given μ, is always higher than the predictions of the EN1993-1-2 formula for $\mu > 3$. Nevertheless, by examining only the predictions of steel temperatures higher than 100°C, it can be observed the EN1993-1-2 predictions are never well positioned in the 0% to + 10% range, in particular for $\mu > 14$. It can be concluded that, for temperatures higher than 100°C the proposed new simple formula improves significantly and becomes always more accurate than the EN1993-1-2 formula for steel temperatures larger than 400°C, for which failure of steel members in fire typically occurs.
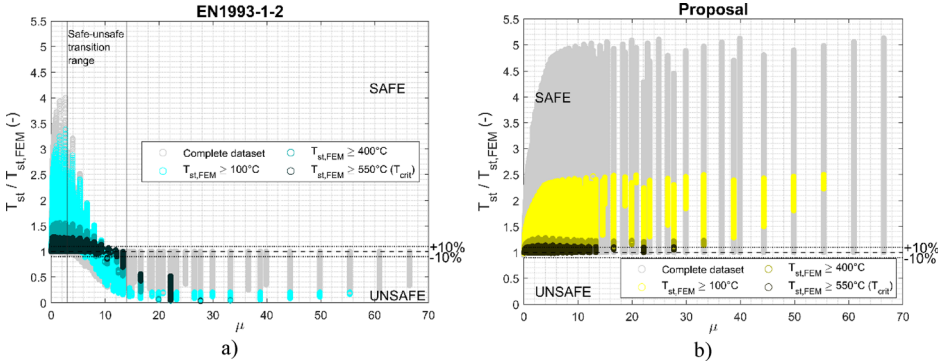
Figure 6. Variation of predicted-numerical temperatures ratio as a function of μ: (a) EN1993-1-2; (b) new formula.

As a further general conclusion, the new formula should be preferred to the one of EN1993-1-2 for heavily insulated steel members, and in particular for $\mu > 14$.

As already mentioned, the less accurate predictions provided by the new simple formula are obtained at low steel temperatures. This is mainly due to the absence of a term that accounts for the time delay t_d. Nonetheless, an additional parameter would entail a more complex formulation and is beyond this work's scope.

3.4. Fire Resistance Classification

In this section, the predictions in terms of fire resistance classification for both analytical formulas will be compared against FE results. Assuming that the fire resistance requirement is met until the temperature does not exceed the critical temperature, taken as $T_{crit} = 550°C$, the numerical analysis results were used to set the actual fire resistance class. For each steel-insulation configuration, the times t_{crit} at which the critical temperature T_{crit} was exceeded were identified. The number in the class label represents the minutes for which the resistance is guaranteed. For instance, the R15 class implies that the steel member can withstand the applied loads for at least 15 min. The fire resistance class was determined as follows: an analysis with $t_{crit} = 58$ min was classified as R45. The fire resistance classes were then predicted from the EN1993-1-2 formula and the new proposal, and were compared with the fire classification obtained from numerical simulations in the two confusion matrices reported in Fig. 7. In these matrices, the diagonal values correspond to the number of correct fire resistance class identifications. This means that the same fire classification was obtained from the analytical formula and the numerical analyses. Conversely, the out-of-diagonal values represent the misclassified fire resistances, where over- and underestimated classes are found above and below the diagonal. The new proposal allows for a better classification as more analyses are located on the diagonal with respect to the EN1993-1-2 formula. The misclassified fire resistances computed with the new formula were consistently below the diagonal on the safe side and never for more than one class (see Fig. 7b). Instead, the misclassified fire resistance classes obtained with the
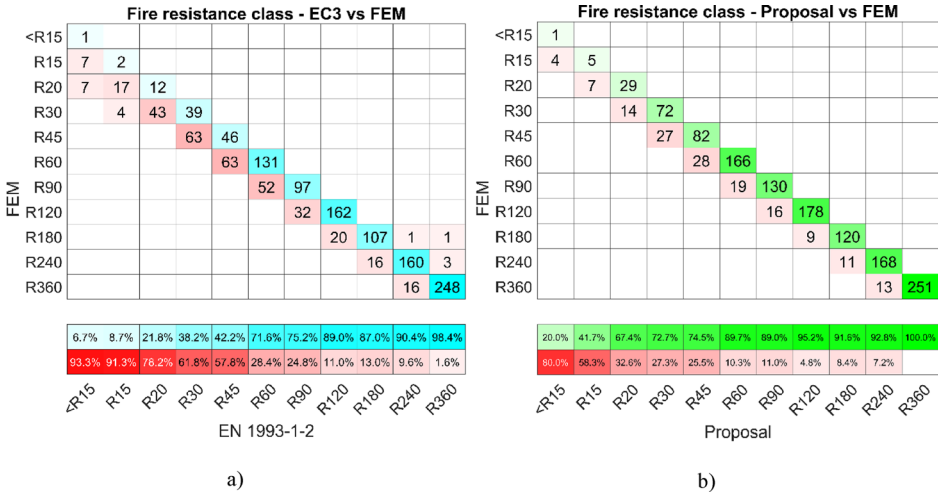
Fire resistance class - EC3 vs FEM

FEM \ EN 1993-1-2	<R15	R15	R20	R30	R45	R60	R90	R120	R180	R240	R360
<R15	1										
R15	7	2									
R20	7	17	12								
R30		4	43	39							
R45				63	46						
R60					63	131					
R90						52	97				
R120							32	162			
R180								20	107	1	1
R240									16	160	3
R360										16	248

6.7%	8.7%	21.8%	38.2%	42.2%	71.6%	75.2%	89.0%	87.0%	90.4%	98.4%
93.3%	91.3%	78.2%	61.8%	57.8%	28.4%	24.8%	11.0%	13.0%	9.6%	1.6%

a)

Fire resistance class - Proposal vs FEM

FEM \ Proposal	<R15	R15	R20	R30	R45	R60	R90	R120	R180	R240	R360
<R15	1										
R15	4	5									
R20		7	29								
R30			14	72							
R45				27	82						
R60					28	166					
R90						19	130				
R120							16	178			
R180								9	120		
R240									11	168	
R360										13	251

20.0%	41.7%	67.4%	72.7%	74.5%	69.7%	89.0%	95.2%	91.6%	92.8%	100.0%
80.0%	58.3%	32.6%	27.3%	25.5%	10.3%	11.0%	4.8%	8.4%	7.2%	

b)

Figure 7. Fire resistance class misclassification for $T_{crit} = 550°C$: (a) EN1993-1-2; (b) new formula.

EN1993-1-2 formula (Fig. 7a) sometimes differed from the classification of numerical analyses for more than one class. Hence, they were not always on the safe side. A too conservative classification was obtained for the lowest classes, while some fire resistance classifications were unsafe for higher classes.

The accuracy of the classifications can be evaluated with a synthetic indicator that spans from 0, when no class is correctly identified, to 1, when all classes are correctly identified. It is defined as the ratio between the sum of the diagonal values and the sum of the diagonal and the off-diagonal values. This indicator assumes the value of 0.74 and 0.89 at $T_{crit} = 550°C$ for the EN1993-1-2 and the new proposal, respectively. The same quantification was performed, varying the temperature threshold with increments of 10°C from 30°C to 900°C and the evolution of the accuracy indicator for the two formulas is reported in Fig. 8. As expected, the classification obtained from the new formula is worse than the one from EN1993-1-2 only for low steel temperatures that are not relevant for structural fire engineering applications. For steel temperatures higher than 400°C, for which the steel yield strength is reduced ($k_y < 1$), the proposal ensures a significantly higher accuracy, with an accuracy indicator value equal to 0.79 at 400°C and 0.99 at 900°C. In the same range, for the EN1993-1-2 formula, the indicator assumes values between 0.69 and 0.89.

4. Validation for 2-D Applications Against Numerical and Experimental Data

In the previous section, the ability of the two simple formulas to predict the steel temperatures in 1-D heat-transfer problems was assessed. However, temperature gradients may establish in protected steel sections, and in some cases, it may not
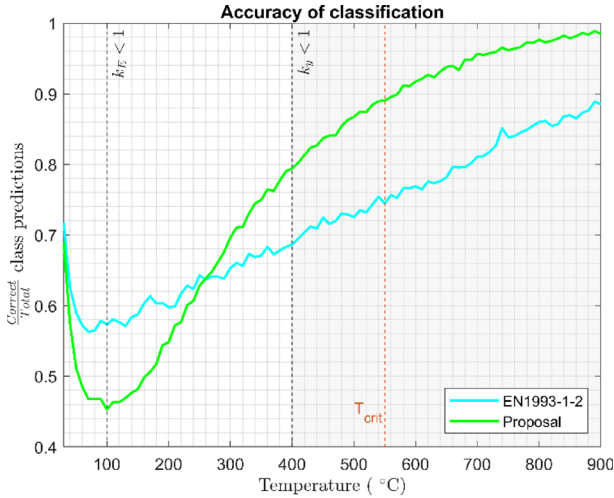
Figure 8. Accuracy of classifications as a function of a selected critical steel temperature.

be easy to refer to a single steel temperature to describe the thermal field. Therefore, the predictions of the EN1993-1-2 formula and the new formula are compared with relevant 2-D numerical and experimental applications. This section validates the proposed new formula against both 2-D numerical analyses and experimental results. The considered protected steel sections are represented in Fig. 9, for both the numerical and the experimental investigations [11–14].

4.1. Numerical 2-D Heat Transfer Analyses

Insulated steel columns exposed on 4 or 3 sides were investigated by means of 2-D FE analyses. Insulation materials characterised by high density were selected to define three different case studies with μ values inside three ranges: (i) $\mu < 3$ lightly insulated cross sections; (ii) transition range $3 < \mu < 14$ and (iii) heavily insulated cross sections $\mu > 14$. The analysed configurations are reported in Table 3. Case study 1 consists of a HE400A steel section covered by 20 mm of sprayed calcareous concrete, while Case studies 2 and 3 consider HE240AA and HE300AA steel sections protected by bricks. A fire exposure of 360 min and a time step of 10 s were considered. The section factor A_{st}/V_{st} of the steel sections was calculated as prescribed in EN1993-1-2 [18] and employed in Equation (7) to compute the parameter μ and in Equation (4) to derive C_{st}. Figure 9a illustrates the 2-D numerical models. For sections exposed on 4 sides, the ISO834 heating curve was applied as boundary condition to the external perimeter of the insulation material. For the 3 sides exposure, the ISO834 heating curve was applied to 3 sides of the cross-section, and an adiabatic condition was imposed on the remaining top face of the section.

The steel temperature T_{st} obtained with the EN1993-1-2 formula and the new proposal are compared with numerical results in Fig. 10. In particular for 3 side
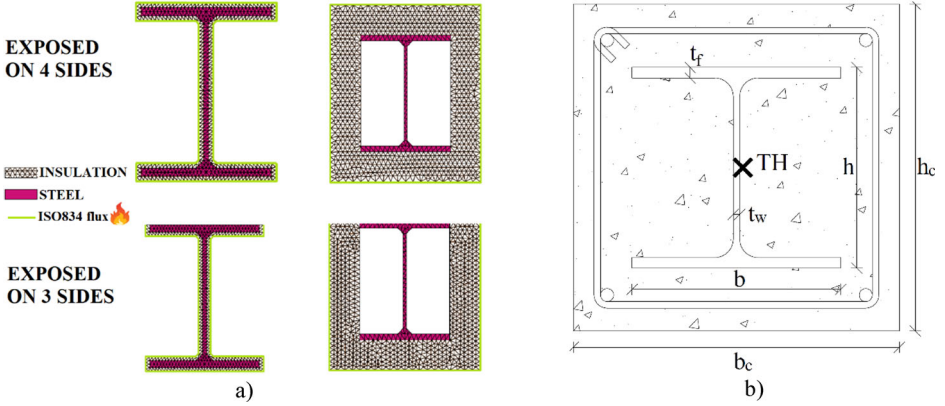
Figure 9. (a) 2-D numerical models for concrete-sprayed and brick-encased sections; (b) concrete-encased sections tested experimentally [11–14].

exposure, non-uniform temperature distribution establish in the cross-sections, and the minimum and the maximum steel temperatures are indicated in Fig. 10. Moreover, also the weighted average steel temperature $T_{st,FEM,AVG}$ is reported in Fig. 10. Assuming that the axial force is the relevant action, which is the case of steel elements employed as compressed or tension members, the weighted average yields

$$T_{st,FEM,AVG} = \left(\sum_{i=1}^{n} A_{st,i} T_{st,FEM,i}\right) / \left(\sum_{i=1}^{n} A_{st,i}\right) \tag{11}$$

where $T_{st,FEM,i}$ and $A_{st,i}$ are the temperature and the area of the i-th steel fibre and n is the total number of steel fibres in the numerical model. Nonetheless, different formulas could be employed to define $T_{st,FEM,AVG}$, for instance, weighting the temperature on the moment of inertia rather than the area of the steel fibres when the bending moment is considered as the dominant action.

In Case study 1, the EN1993-1-2 formula gives similar but higher temperatures than the new formula, as depicted in Fig. 10a and Fig. 10b. $T_{st,EN1993-1-2}$ overestimates the numerical results, whilst the new formula ($T_{st,Proposal}$) tends to provide more accurate predictions between $T_{st,FEM,AVG}$ and the maximum steel temperature. Results of Case study 2, shown in Fig. 10c, d, confirm that for $3<\mu<14$ the EN1993-1-2 predictions might be both safe and unsafe. In detail, $T_{st,EN1993-1-2}$ is always lower than $T_{st,FEM,AVG}$ for 4 sides exposure and until 250 min for 3 sides exposure. The new formula gives safe steel temperature predictions being always higher than $T_{st,FEM,AVG}$. For Case study 1 and 2 and for steel temperatures between 400°C and 800°C, the new formula always provides higher predictions with respect to the average FE steel temperature. Finally, Case study 3 shows that the EN1993-1-2 predictions are unsafe for $\mu>14$, but an evident worsening of steel temperature predictions might appear already at lower ratios, as for $\mu=12.95$ and 3 sides exposure. In particular, $T_{st,EN1993-1-2}$ never increased beyond 20°C in the

Table 3
Investigated Insulated Steel Sections – 2-D Analyses

| Case study | Steel section | h (mm) | b (mm) | t_w(mm) | t_f(mm) | A_{st}/V_{st}(m^{-1}) | | | Insulation material (Properties in Table 1) | d_{in}(mm) | μ(-) | |
						4 sides	3 sides				4 sides	3 sides
1	HE400A	390	300	11	19	120	101		Calcareous concrete	20	1.76	1.48
2	HE240AA	224	240	6.5	10.5	154	114		Bricks	100	10.21	7.57
3	HE300AA	283	300	7.5	10.5	131	97.4		Bricks	200	17.43	12.95
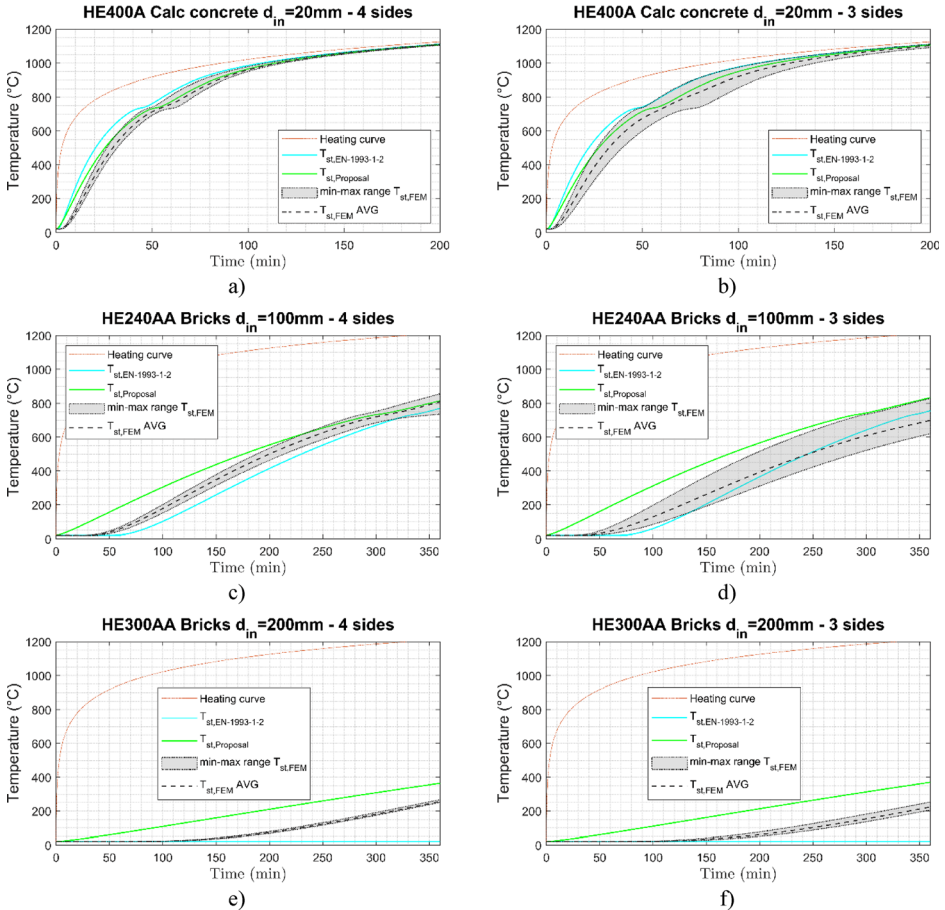
Figure 10. **Numerical vs predicted steel temperatures. (a) Case study 1 exposure on 4 sides; (b) Case study 1 exposure on 3 sides; (c) Case study 2 exposure 4 sides; (d) Case study 2 exposure 3 sides; (e) Case study 3 exposure on 4 sides; (f) Case study 3 exposure on 3 sides.**

360 min of fire exposure; thus, it is out of its validity range. Conversely, the proposed new formula is always safe and provides better and quite conservative temperature estimates, which is in line with the analytical nature of the formula. It is also worth noting that with such heavy insulation, very low temperatures are attained after 360 min, that in most cases, should not endanger the capacity of a steel element. Table 4 compares the times at which the EN1993-1-2, the new formula and the FE analyses attain the temperature values of 100°C, 400°C and 550°C. The EN1993-1-2 formula is safe only in Case study 1. Conversely, the new formula is always safe, particularly for Case studies 2 and 3 when a heavy insulation is employed.

Table 4
Times at Which Relevant Temperatures are Attained – 2-D Analyses

| Case study | T_{st} | Time t (min) | | | | | |
| | | FEM AVG | | EN1993-1–2 | | Proposal | |
		4 sides	3 sides	4 sides	3 sides	4 sides	3 sides
1	100℃	9	9	5	5	5	5
2		76	88	99	116	31	31
3		228	247	> 360	> 360	91	89
1	400℃	24	26	15	17	19	21
2		166	203	195	211	135	132
3		> 360	> 360	> 360	> 360	> 360	> 360
1	550℃	33	36	24	25	29	31
2		218	269	249	263	198	193
3		> 360	> 360	> 360	> 360	> 360	> 360

4.2. *Experimental Data*

This section performs validation of the new formula against experimental data. Fire tests performed on encased steel sections (see Fig. 9) were selected [11–14] to investigate the ability of the analytical formulas to predict the steel temperature within heavily-insulated sections characterised by a μ value higher than 12. Specimens subjected to the ISO834 heating curve were tested by Han et al. [11] and Rodrigues et al. [12], while Huang et al. [13, 14] performed tests in which the furnace temperature was increased according to linear ramps, as shown in Fig. 11. Experimental outcomes that were obtained according to a very short fire exposure [11] or that differed significantly from numerical analyses as in [13] were not considered. Hence, two tests from Han et al. [11] and Huang et al. [14], and one test from Rodrigues et al. [12] and from Huang et al. [13] were selected, as shown in Table 5. While the density of concrete ρ_{in} employed in each work was given, no indication about the thermal properties of concrete was provided. Thus, in the predictive equations c_{in} and λ_{in} were assumed equal to 1100 J/kgK and 1.3 W/mK, respectively. The steel properties were assumed according to EN1993-1-2. For each test, the geometric dimensions of the steel section and the square concrete encasement, as well as the values of the parameter μ are reported in Table 5. Experimental temperatures measured through thermocouples installed on the web surface at its mid-height (see Fig. 9b) are compared with the temperature estimates of the predictive equations in Fig. 11. Therefore, the thickness of insulation employed in the predictive equations and reported in Table 5 is obtained as $d_{in} = (b_c - t_w)/2$.

Figure 11 shows that compared with the EN1993-1-2, the new formula better reproduces the experimental results, particularly for tests performed when the ISO834 heating curve was applied. Indeed, a very good agreement between the new formula and the experimental data is found. Furthermore, the new formula gives predictions that are always safer or slightly lower than the EN1993-1-2 ones. Thus, this confirms that the it can provide safer and better predictions in a wider
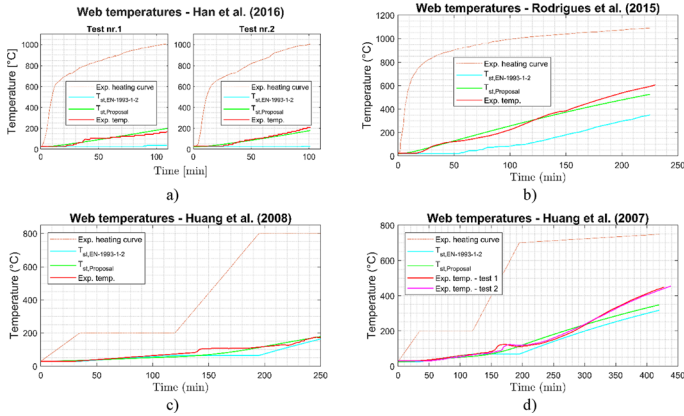
Figure 11. Experimental vs predicted temperatures on the web surface of encased steel sections. (a) Han et al. [11]; (b) Rodrigues et al. [12]; (c) Huang et al. [13]; (d) Huang et al. [14].

Table 5
Investigated Encased-Steel Sections – Experimental Tests

Tests	h (mm)	b (mm)	t_w(mm)	t_f(mm)	A_{st}/V_{st}(m^{-1})	b_c = h_c(mm)	d_{in}(mm)	μ(−)
Han et al. [11]	150	150	9.3	9.3	150	300	145	16.61
Rodrigues et al. [12]	152	152	6.0	9.0	169	250	123	14.60
Huang et al. [13]	254.1	254.6	8.6	14.2	109	350	171	12.50
Huang et al. [14]	161.8	154.4	8.0	11.5	134	300	146	14.97

range than the EN1993-1-2 formula. This is particularly true for heavily protected steel sections.

5. Conclusions

The paper proposed a new simple analytical formula to predict the steel temperature based on the mass lumped approach that widens the applicability field to heavily protected steel cross sections. In fact, the simple formula included in the current version of EN1993-1-2 assumes that the temperature of the exposed surface equals the temperature of the surrounding gas. Still, it was demonstrated to be inaccurate for insulation materials with relatively high heat capacity. Conversely, the new formula is based on more realistic heat flux boundary conditions that allow for convection and radiation terms, and it is suited for materials with high heat capacity. For validation purposes, a parametric analysis consisting of 1-D heat-transfer finite element analyses was carried out, whose outcomes were

compared with the predictions of the new formula and the EN1993-1-2 formula. The results showed that the new formula always ensures safe or only slightly unsafe predictions. In greater detail, the predicted temperatures were rarely lower than the numerical temperatures, assumed as the maximum temperatures in the steel sections, and never by more than 10%. On the contrary, the EN1993-1-2 formula gives both safe and unsafe predictions. It is significantly unsafe for heavily protected sections that are characterised by high μ values, which is the ratio between the heat capacity of the insulation and the steel. In particular, predictions move from safe when $\mu<3$ to unsafe when $\mu>14$. Considering only temperatures above relevant thresholds for steel mechanical property degradation, such as 100°C or 400°C, the predictions obtained with the proposed new formula improve significantly and fit very well the safe 0% to $+10\%$ range when steel temperatures above 550°C are considered. In particular, the new formula RMSE (root mean squared error) significantly decreases when the steel temperature is above 100°C, while for the EN1993-1-2, the RMSE remains almost constant. The new formula was also sufficiently accurate and safe-sided when compared against 2-D numerical analyses of H-shaped steel sections. In the three investigated case studies, predictions were never lower than the numerical steel temperature in the cross-section. Conversely, the EN1993-1-2 showed to be less accurate and too conservative or unsafe. Moreover, the new proposal could reproduce with good approximation the experimental steel temperature evolution of the encased steel sections tested in four different experimental campaigns. Again, the EN1993-1-2 formula failed to provide sufficiently accurate estimates for heavily-insulated cross sections. As a general indication, the new simple formula can be employed regardless of the value of μ, but is particularly recommended for heavily insulated steel members, especially for $\mu>14$. In future developments, the proposed new formula could be further improved by introducing a term to account for the initial time delay to reduce the initial overestimate of the steel temperatures.

Declarations

Conflict of interest The authors declare that there are no conflicts of interest.

Ethical Approval No human participants or animals were involved in the research.

Informed consent No human participants or animals were involved in the research.

Open Access

References

1. Possidente L, Weiss A, de Silva D, Pustorino S, Nigro E, Tondini N (2021) Fire safety engineering principles applied to a multi-storey steel building. Proc Inst Civ Eng Struct Build 174(9):725–738
2. Covi P, Tondini N, Sarreshtehdari A, Elhami-Khorasani N (2023) Development of a novel fire following earthquake probabilistic framework applied to a steel braced frame. Struct Saf . 10.1016/j.strusafe.2023.102377
3. National Institute of Standards and Technology – NIST (2004) Fire protection of structural steel in high-rise buildings
4. Leborgne H, Thomas L (1999) Techniques de protections rapportées des structures en acier. Constr Met (CTICM) 3:123–135
5. Mariappan T (2016) Recent developments of intumescent fire protection coatings for structural steel : a review. J Fire Sci 34(2):120–163
6. de Silva D, Bilotta A, Nigro E (2019) Experimental investigation on steel elements protected with intumescent coating. Construct Build Mater 205:232–244
7. Keerthan P, Mahendran M (2012) Numerical studies of gypsum plasterboard panels under standard fire conditions. Fire Saf J 53:105–119
8. Fulmer GE (1982) Method of making a fire-retardant product having a foamed lore and a fire-retardant protective layer, 1982. US 4349494

9. Zhang Q, Li VC (2015) Development of durable spray-applied fire-resistive engineered cementitious composites (SFR-ECC). Cement Concr Compos 60:10–16

10. Randaxhe J, Popa N, Vassart O, Tondini N (2021) Development of a plug-and-play fire protection system for steel column. Fire Saf J 121:103272

11. Han L-H, Zhou K, Tan Q-H, Song T-Y (2016) Performance of steel-reinforced concrete column after exposure to fire: FEA model and experiments. J Struct Eng 142:9

12. Rodrigues JPC, Correia AJM, Pires TAC (2015) Behaviour of composite columns made of totally encased steel sections in fire. J Construct Steel Res 105:97–106

13. Huang Z-F, Tana K-H, Tohb W-S, Phnga G-H (2008) Fire resistance of composite columns with embedded I-section steel—effects of section size and load level. J Construct Steel Res 64:312–325

14. Huang Z-F, Tana K-H, Phnga G-H (2008) Axial restraint effects on the fire resistance of composite columns encasing I-section steel. J Construct Steel Res 63:437–447

15. Possidente L, Tondini N, Battini J-M (2019) Branch-switching procedure for post-buckling analyses of thin-walled steel members in fire. Thin Walled Struct 136:90–98

16. Possidente L, Tondini N, Battini J-M (2020) 3D beam element for the analysis of torsional problems of steel-structures in fire. J Struct Eng. 10.1061/(ASCE)ST.1943-541X.0002665

17. Wickström U (1985) Temperature analysis of heavily-insulated steel structures exposed to fire. Fire Saf J 9:281–285

18. European Comitee for Standardisation (2005) Eurocode 3 design of steel structures—part 1–2: general rules—structural fire design

19. European Comitee for Standardisation (2005) Eurocode 4 design of composite steel and concrete structures - part 1–2: general rules—structural fire design

20. ECCS Technical Committee 3 (1983) European recommendations for the fire safety of steel structures. Amsterdam: Elsevier Scientific Publishing Company

21. Melinek SJ, Thomas PH (1987) Heat flow to insulated steel. Fire Saf J 12:1–8

22. Wang Z-H, Kang HT (2006) Sensitivity study of time delay coefficient of heat transfer formulations for insulated steel members exposed to fire. Fire Saf J 41:31–38

23. Wong MB, Ghojel JI (2003) Sensitivity analysis of heat transfer formulations for insulated structural steel components. Fire Saf J 38:187–201

24. Possidente L, Tondini N, Wickström U (2023) Derivation of a new temperature calculation formulation for heavily fire insulated steel cross-sections. Fire Saf J 141:103991. https://doi.org/10.1016/j.firesaf.2023.103991

25. Siegel R, Howell J (1972) Thermal radiation heat transfer. McGraw-Hill Book Company,

26. Incropera FP, DeWitt DP (1996) Fundamentals of heat and mass transfer. Wiley, Hoboken

27. Holman JP (2009) Heat transfer, 10 edn. McGraw Hill, New York

28. Franssen JM, Gernay T (2017) Modeling structures in fire with SAFIR: theoretical background and capabilities. J Struct Fire Eng 8(3):300–323

29. UNI 9503 (2003) Procedimento analitico per valutare la resistenza al fuoco degli elementi costruttivi di acciaio, Ente Nazionale Italiano di Unificazione, Milano

30. Ministry of Interior, Italian Government (2015) Norme tecniche di prevenzione incendi, gazzetta ufficiale n. 192 del 20 agosto 2015

31. Franssen JM, Schleich JB, Cajot LG (1995) A simple model for the fire resistance of axially-loaded members according to eurocode 3. J Constr Steel Res 35:49–69

32. Couto C, Vila Real P, Lopes N, Zhao B (2015) Resistance of steel cross-sections with local buckling at elevated temperatures. J Construct Steel Res 109:101–114

33. Possidente L, Tondini N, Battini JM (2022) Torsional and flexural-torsional buckling of compressed steel members in fire. J Construct Steel Res 171:106130